COBEM 2023 27TH INTERNATIONAL CONGRESS OF MECHANICAL ENGENEERING

ABCM Brazilian Society of Mechanical Sciences and Engineering
27th ABCM International Congress of Mechanical Engineering
December 04-08, 2023, Florianópolis-SC, Brazil

COB-2023-1073
STUDY OF THE INFLUENCE OF THE FILM HEIGHT ON NEAR-INTERFACE TURBULENT STRUCTURE IN GAS-LIQUID STRATIFIED FLOW VIA DNS

Victor W. F. de Azevedo
Department of Engineering and Technology, Federal Rural University of the Semiarid Region, 59625-900, Mossoró-RN, Brazil
victorwfreire@ufersa.edu.br

Fabian Denner
Department of Mechanical Engineering, Polytechnique Montréal, Montréal, H3T 1J4, QC, Canada
fabian.denner@polymtl.ca

Emilio E. Paladino
Department of Mechanical Engineering, Federal University of Santa Catarina, 88040-900, Florianópolis-SC, Brazil
emilio.paladino@ufsc.br

Abstract. *Stratified gas-liquid flows are present in several applications in nature and industrial processes. In such flows, the near-interface turbulence structure is important as is the region responsible for mass, momentum, and energy transfer between the phases. In flow with high Reynolds numbers, the turbulence phenomena in this region governs friction pressure loss and heat and mass diffusion, as well as it affects the onset of interfacial wave formation and, eventually, pattern transition. Despite the availability of turbulence models with different levels of detail and assumptions, the direct numerical simulation is still a useful tool for fundamental studies in many flows. Furthermore, for the case of turbulent flows in the presence of fluid-fluid interfaces, typical turbulence models are based on modifications of those developed for single phase flow and normally application based with adjustable parameters. Some previous works studied the turbulence in the near-interface region in stratified flows but did not consider the influence of the wall in near-interface turbulence statistics, as the developed models typically include only the interface region and not the actual wall-bounded stratified channel flow. In the present work, considering a computational domain bounded by no-slip walls, we show that near-interface turbulence structure is affected by the presence of walls by performing DNS of stratified channel flow considering different film heights. The model is developed in a second order finite volume framework for the flow in a wall-bounded gas-liquid stratified flow with different film heights considering the volume-of-fluid model for the advection of volume fraction. The results show increasing in interfacial friction factor and decreasing in turbulence production for the smaller film height with relation to the bigger film height, which leads to conclusion that not only the interface deformation but also the distance of the interface to the wall affects the turbulence structure in the near-interface region.*

Keywords: *stratified flow, Direct Numerical Simulation (DNS), near-interface turbulence.*

1. INTRODUCTION

Multiphase flows have many applications in general phenomena in nature and industry, where the stratified flow pattern is one which happens most. Allied with such theme, turbulence is also highly present in daylife phenomena and its complexity is still theme for studies in the present time. Considering internal flows, the wall region has strong influence in the turbulence behaviour, however, in stratified flows, the gas-liquid interface region has also great importance. This referred region is responsible for transfer mechanism of mass and momentum between the phases, which, with the wall region, are responsible for the main influence in turbulence structure of internal multiphase flows.

Turbulence can be modelled, which provide good results for complex cases (Frederix *et al.*, 2018), however, the direct numerical simulation (DNS) of turbulence, even computationally heavy, can provide very detailed data about flow behaviour which can be applied nowadays, for instance, in the training of neural networks (Le Clainche *et al.*, 2023).

The onset of near-interface turbulence studying with DNS is credited to Lombardi *et al.* (1996) and De Angelis *et al.* (1997), which performed DNS for the near-interface region in the stratified flow considering a flat interface and a wavy non-deformable interface, respectively. These works were the basis for the development of a model which considers a deformable interface by Fulgosi *et al.* (2003). This work concluded that the turbulence statistics of the stratified flow in the gas phase resembles the near-wall's statistics for a single-phase flow, even though, a certain damping was observed in the near-interface region against the near-wall region. The obtained results allowed the proposition of a damping function by Lakehal *et al.* (2005) which later was satisfactory tested by Liovic and Lakehal (2007), correctly predicting the flow

behaviour compared with the DNS results.

The influence of film height in turbulence statistics of wall-bounded flows was not deeply studied in literature. The work of Chongsiripinyo and You (2018) analysed different interface positions in gas-liquid flow, however, they only considered the influence of liquid phase in turbulence statistics. Additionally, Bender *et al.* (2019) characterized the film dynamics based on a gas-liquid stratified flow through DNS, which lead to conclusion that turbulent shear stress fluctuations have high impact in film shape.

Based on these works, even though stratified flow have been studied vastily, some additional knowledge of interface influence in turbulence statistics still need complementation. Hence, the present work performed DNS for stratified flow considering different film heights, in order to obtain the influence of interface position in turbulence statistics also considering the presence of walls in the computational domain.

The general model set-up for stratified flow is described in Section 2.which include the adopted computational meshes and boundary conditions. The processed data are shown and discussed in Section 3for both flows and finally the conclusions and future works suggestions are made in Section 4.

2. COMPUTATIONAL MODEL

2.1 Governing equations

Momentum equations for the incompressible flow

$$\frac{\partial \rho u_i}{\partial t} + \frac{\partial (\rho u_j u_i)}{\partial x_j} = -\frac{\partial p}{\partial x_i} + \frac{\partial}{\partial x_j}\left[\mu\left(\frac{\partial u_i}{\partial x_j} + \frac{\partial u_j}{\partial x_i}\right)\right] + \rho g \tag{1}$$

where, u_i denote fluid velocity components, p the pressure, t denotes physical time, ρ denotes fluid density and μ denotes fluid viscosity; are discretized following the second-order finite volume method. The Volume of Fluid (VOF) method is applied for interface capture, hence, the fluid properties are approached as

$$\rho = \alpha\rho_L + (1-\alpha)\rho_G \tag{2}$$

and

$$\mu = \alpha\mu_L + (1-\alpha)\mu_G \tag{3}$$

where α is the volume fraction and the subscripts *G* and *L* denote the gas and liquid phases, respectively. The volume fraction is advected through the domain following the CICSAM scheme (Ubbink and Issa, 1999) and the height-function (HF) method (López *et al.*, 2009) is used to calculate the curvature radii.

2.2 Model set-up

Stratified gas-liquid flow with different film heights was considered in the present work with $Re_\tau \approx 180$ for both phases. The problem is solved in a VOF-framework which consirers a pressure-based solver and coupled solution (Denner and van Wachem, 2014). The computational domain is bounded by no-slip walls in the y-direction (normal direction) and by periodic boundaries in the x- and z-directions (stream- and span-wise directions, respectively).

The considered film heights for the present case were 2δ and δ, where δ is the turbulent integral scale. The computational box for the cases are presented in Tab. 1 with the respective computational mesh for each phase, where

$$\phi^+ = \frac{\Delta\phi u_{\tau_L}}{\nu_L} \tag{4}$$

based on the respective ϕ direction (x for stream-wise, y for normal and z for span-wise directions). In Eq. 4, ν_L is the kinematic viscosity of the liquid phase, u_{τ_L} is the friction velocity of the liquid phase

$$u_{\tau_L} = \sqrt{\frac{\tau_{w_L}}{\rho_L}}, \tag{5}$$

where ρ_L is the density of the liquid phase and τ_{w_L} is the shear stress in the wall region of the liquid side.

The flow is driven in the stream-wise direction by a constant pressure gradient of

$$\frac{\Delta p}{\Delta x} = \frac{Re_{\tau_L}\nu_L^2\rho_L}{\delta^3}, \tag{6}$$

Case	**Box size**	N_x **x** N_y **x** N_z	x^+	y_c^+	z^+
$\delta_f = 2\delta$ gas	12δ x 2δ x 6δ	512 x 128 x 128	4.41	2.81	8.83
$\delta_f = 2\delta$ liquid	12δ x 2δ x 6δ	512 x 128 x 128	4.30	2.74	8.61
$\delta_f = \delta$ gas	12δ x 2δ x 6δ	512 x 128 x 128	4.41	2.81	8.83
$\delta_f = \delta$ liquid	12δ x δ x 6δ	512 x 64 x 128	4.30	2.74	8.61

Table 1: Mesh statistics for the both film heights cases obtained *a priori*. Note that the gas phase domain is the same for both cases, only the liquid phase domain is changed from 2δ to δ.

for the 2δ case, and,

$$\frac{\Delta p}{\Delta x} = \frac{Re_{\tau_L}\nu_L^2\rho_L}{8\delta^3}, \tag{7}$$

for the δ case, where $Re_{\tau L}$ is the friction-velocity based Reynolds number for the liquid phase

$$Re_{\tau_L} = \frac{u_{\tau_L}\delta}{\nu_L}. \tag{8}$$

Equations 6 and 7 were obtained based on the interfacial coupling between both phases $\tau_{I_L} = \tau_{I_G}$, where τ_I is the interfacial shear stress for the respective G gas and L liquid phases. According to Chongsiripinyo and You (2018), only the liquid phase must be considered in the analysis of the pressure gradient due to scalling reasons, once the pressure gradient should only counteract the liquid phase shear stress.

The surface tension coefficient σ is considered in this model based on the Froude and Weber numbers

$$\text{Fr} = \frac{u_{\tau_L}^2\rho_L}{g\delta(\rho_L - \rho_G)} \tag{9}$$

$$\text{We} = \frac{\rho_L\delta u_{\tau_L^2}}{\sigma} \tag{10}$$

where the relation $\sqrt{\text{Fr}}/\text{We} = 1.4$ is applied as is established to be in the the capillary wave regime (Zonta *et al.*, 2016).

The initial tests with the stratified flow case showed that the phases must be simulated separately and then merged into one single domain to avoid interface break-up. Hence, DNS were performed for the gas and liquid phases separately following the validated methodology for the single-phase and stratified flows (de Azevedo *et al.*, 2021; de Azevedo and Paladino, 2022). Based on the already known behaviour of the gas phase, which "sees" the interface as a no-slip wall (Fulgosi *et al.*, 2003), a wall-bounded domain was considered when performing DNS for this phase, however, for the liquid phase, a freeslip boundary was considered in the top part of the domain and a no-slip wall was considered in the bottom part. After the velocity fields are developed, they are merged into one single domain – the stratified flow domain. The merged computational domain represents a wall-bounded section of the stratified flow with different film heights, both presented in Fig. 1, which is showing the initial velocity field for the gas (top part) and liquid (bottom part) phases for the 2δ film height (see Fig. 1a) and δ film height (see Fig. 1b).

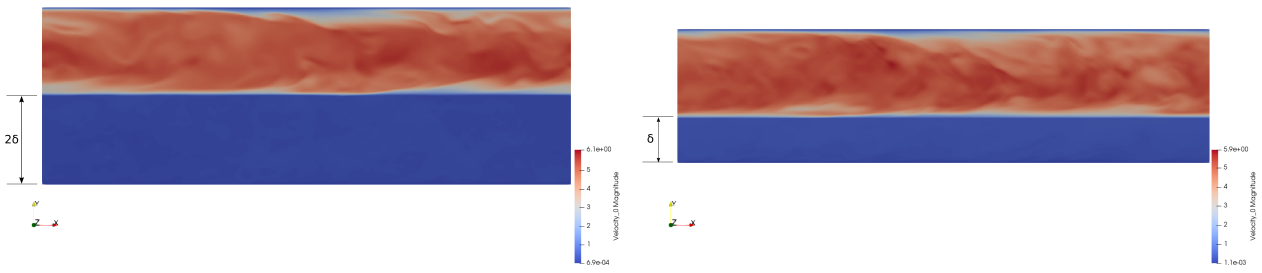

(a) (b)

Figure 1: Initial velocity fields for: (a) 2δ film height case and (b) δ film height case.

3. RESULTS

The obtained results are presented in this section for both film heights. The results for the stratified flow were compared to previous results for the near-wall turbulence in the single-phase flow of de Azevedo *et al.* (2021) and stratified flow of de Azevedo and Paladino (2022).

3.1 Velocity fluctuations

Velocity fluctuations are obtained following the classic Reynolds decomposition of flow velocity

$$u_i = \langle u_i \rangle + u_i', \tag{11}$$

where u_i is the instant component of the velocity, u_i' the velocity fluctuation component and the brackets present the average of the velocity field.

Results for the velocity-rms fluctuations are presented in Fig. 2 for both film heights compared to the single-phase flow DNS results. The stream-wise results for both film heights remained close to the single-phase near-wall behaviour, however, some small differences can be noted in normal and span-wise components for the smaller film height case, which smaller obtained values suggest a certain damping in the turbulence in this region.

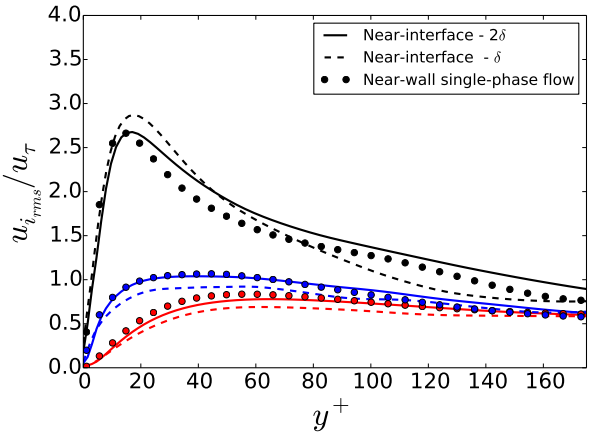

Figure 2: Stream-wise (black), normal (blue) and span-wise (red) components of the velocity-rms fluctuations for the: (-) near-interface 2δ film height case and (- -) near-interface δ film height case. The dots present the near-wall single-phase flow case.

3.2 Autocorrelation functions

The autocorrelation functions of the velocity fluctuation components are expressed as (Pope, 2001; Trofimova *et al.*, 2009)

$$R_{ii}(\mathbf{r}, t) = \frac{\langle u_i'(\mathbf{x}+\mathbf{r}, t)\, u_i'(\mathbf{x}, t)\rangle}{\langle u_i' u_i'\rangle}, \tag{12}$$

which is obtained in a y-constant plane of $y^+ \approx 5$, in the near-interface region. At this point, once the DNS is developed in a VOF-framework, is convenient to explain about interface capture. The volume fraction α of the gas phase is tracked in the normal direction and, at the coordinate point where $0 < \alpha < 1$, the interface region is established and an interface film height in obtained. Once the VOF model allows interface deformation, this procedure is followed for all cells in the stream- and span-wise directions, thus, after an averaging process, a mean interface height is obtained. The cell just above the obtained mean height is considered to be the first cell in the gas phase, from where the y^+ reference is obtained for the near-interface region.

The stream-wise autocorrelation functions are presented in Fig. 3 for both film heights compared to the near-wall results of de Azevedo *et al.* (2021), obtained in a similar y^+. The results show a wall-like behaviour for both film heights in all velocity fluctuations components when compared to the single-phase flow.

Although, some small differences between near-wall and -interface behaviours are present when the span-wise auto-correlation functions are analysed (see Fig. 4). The δ film height results remained closer to single-phase flow results than 2δ film height in all components, which leads to conclusion that the influence of the bottom wall in the interface shear stress is enhanced for the smaller film height.

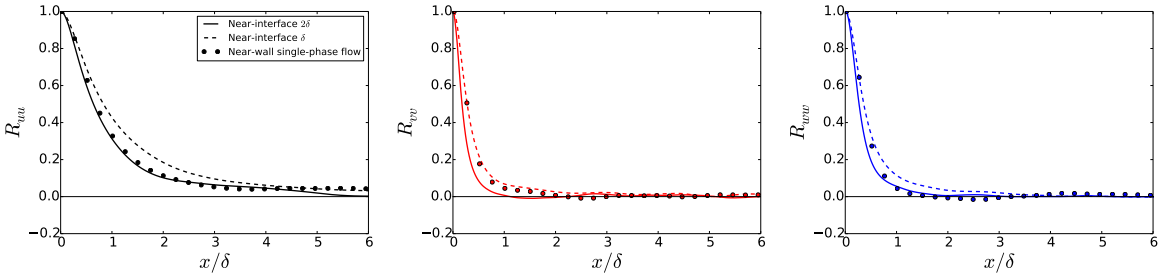

(a) (b) (c)

Figure 3: Autocorrelation functions in the stream-wise direction in the near-interface region compared to the near-wall single-phase flow based on the: (a) stream-wise fluctuation component, (b) normal fluctuation component and (c) span-wise fluctuation component.

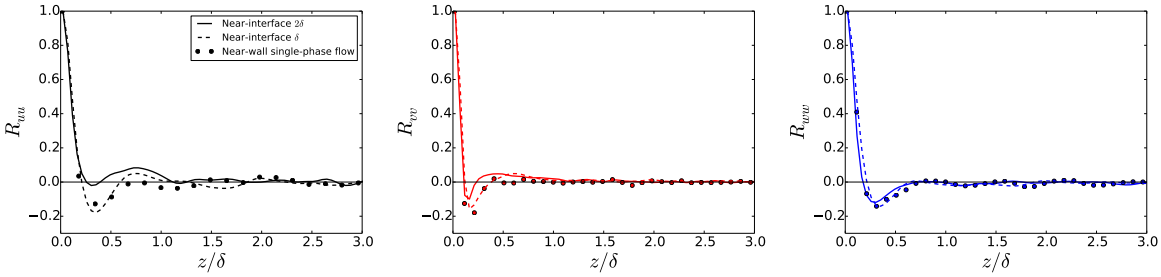

(a) (b) (c)

Figure 4: Autocorrelation functions in the span-wise direction in the near-interface region compared to the near-wall single-phase flow based on the: (a) stream-wise fluctuation component, (b) normal fluctuation component and (c) span-wise fluctuation component.

3.3 One dimentional energy spectrum

The one dimentional energy spectrum in the present work was obtained based in the discrete cosine transform of the autocorrelation functions (Pope, 2001; Trofimova *et al.*, 2009)

$$E_{ij} = \frac{2}{\pi} \int_0^x R_{ij}\left(r_i\right) cos\left(\kappa_i r_i\right) dr_i, \tag{13}$$

where κ is the wavenumber in the respective periodic direction and R_{ij} is the autocorrelation function of the respective velocity fluctuation.

The one dimentional energy spectrum is shown in Fig. 5 for both film heights in the stratified flow and the results were compared to the single-phase flow DNS of Moser *et al.* (1999) for the near-wall region. The results for all components resembles the wall-like behaviour, including the dissipative scale.

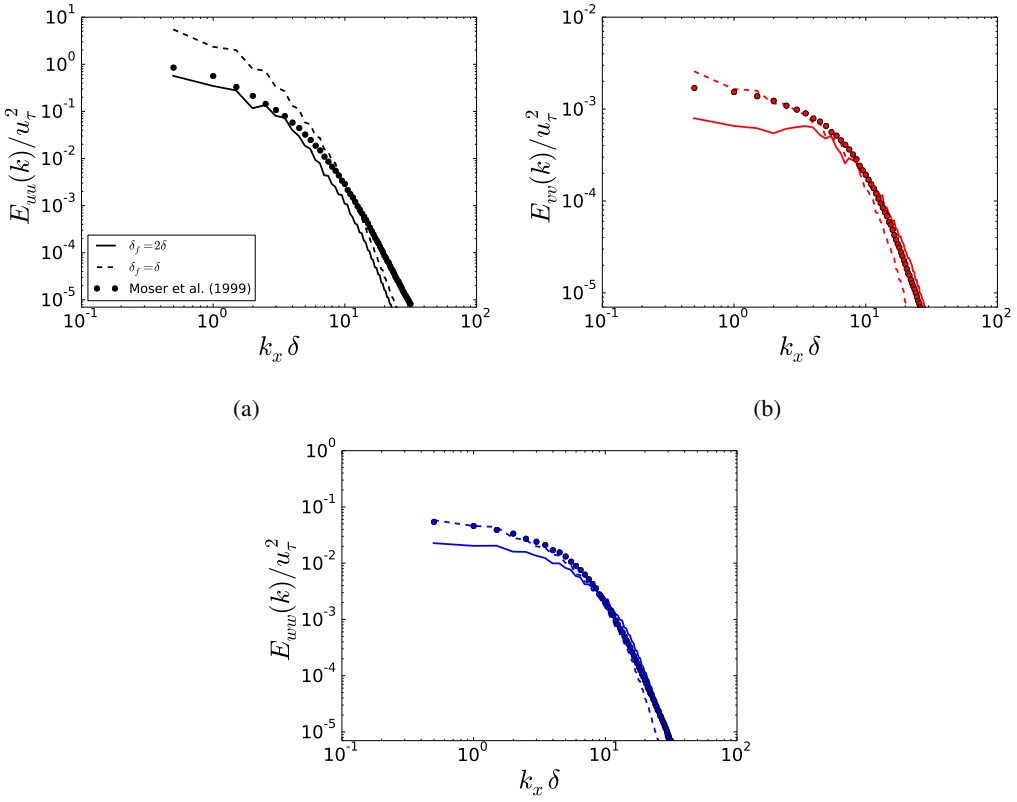

Figure 5: One-dimentional energy spectrum for (-) 2δ case and (- -) δ case for the: (a) stream-wise component, (b) normal component and (c) span-wise component of the autocorrelation functions in the stream-wise direction. The dots represent the results of the DNS of Moser *et al.* (1999).

3.4 Interfacial friction factor

For the analysis of the interfacial friction factor, the correlation of Petalas and Aziz (2000) for stratified flows was used,

$$f_i = \left(0.004 + 0.5 \cdot 10^{-6} Re_{\tau_L}\right) Fr^{1.335} \left(\frac{\rho_L \delta g}{\rho_G u_G^2}\right), \tag{14}$$

This referred correlation was analysed in the work of Abegunde *et al.* (2019) and showed minor errors with relation to experiments and other correlations.

For validation, the correlation obtained in the experiments of Hudaya *et al.* (2018)

$$f_i = 0.0472\eta^{-0.4427} Re_L^{0.2415} Re_G^{-0.0706} \tag{15}$$

was used for comparison, where

$$\eta = 0.016 \left(\frac{u_L}{u_G}\right)^{0.220} Fr_G^{-0.861}, \tag{16}$$

and Fr_G is the Froude number defined as

$$Fr_G = \left[\frac{\rho_G}{\rho_L - \rho_G}\right]^{1/2} \frac{u_G}{(g\delta_G)^{1/2}}. \tag{17}$$

Equations 14 and 15 were used for validation of the interfacial friction factor in the present model for the $\delta_f = 2\delta$ and $= \delta$ cases, as shown in Tab.2, which showed good agreement. The results suggest that the proximity of the wall in the smaller film height results in a higher friction factor in the near-interface region. The aplication of Eq. 15 for the smaller film height case did not presented satisfactory results, a further investigation is necessary regarding the scope of the referred model for smaller film heights.

Case	Present Work	Eq. 14	Eq. 15	% Aprox. Error
$\delta_f = 2\delta$	0.01075	0.01149	0.01135	5.86
$\delta_f = \delta$	0.02096	0.02232	—	6.09

Table 2: Results for the interfacial friction factor obtained in the present work compared to different methodologies.

4. CONCLUSIONS

The present work performed DNS for stratified flow considering different film heights in a VOF-framework with low-order discretization of the governing equations in a wall-bounded domain. The near-interface flow statistics were obtained, which showed a wall-like behaviour in stream-wise velocity fluctuations and stream-wise autocorrelation functions for both film heights. The span-wise autocorrelation functions showed that the smaller film height suffers more influence from the wall region than the bigger film height, which can also be seen in normal and span-wise velocity fluctuations components.

The interfacial friction factor was analysed and it was shown that the smaller film height present higher value than the bigger one, which was also validated with interfacial friction factor models established in literature. These values also suggested that a damping in turbulence is present in the near-interface region, which is increased by the proximity of the interface to the wall.

Although DNS is performed with high-order discretization of governing equations with spectral methods, the current methodogy obtained satisfactory results for stratified flow case considering interface deformation and a wall-bounded domain, which leaves space for more studies regarding interface deformation in more complex domains.

5. ACKNOWLEDGEMENTS

The authors acknowledge the National Laboratory for Scientific Computing (LNCC/MCTI, Brazil) for providing HPC resources of the SDumont supercomputer, which have contributed to the research results reported within this paper.

References

Abegunde, M., Briggs, T., Abam, F. and Awolola, T., 2019. "Evaluation of interfacial friction models in stratified flow: Gas-liquid two-phase flow". In *SPE Nigeria Annual International Conference and Exhibition*. OnePetro.

Bender, A., Stroh, A., Frohnapfel, B., Stephan, P. and Gambaryan-Roisman, T., 2019. "Combined direct numerical simulation and long-wave simulation of a liquid film sheared by a turbulent gas flow in a channel". *Physics of Fluids*, Vol. 31, No. 2, p. 022103.

Chongsiripinyo, K. and You, D., 2018. "Effects of the interface position of water-air flow on turbulent wall structures". *Journal of Mechanical Science and Technology*, Vol. 32, No. 2, pp. 689–695.

De Angelis, V., Lombardi, P. and Banerjee, S., 1997. "Direct numerical simulation of turbulent flow over a wavy wall". *Physics of Fluids (1994-present)*, Vol. 9, No. 8, pp. 2429–2442.

de Azevedo, V.W.F. and Paladino, E.E., 2022. "Dns of gas-liquid stratified flow using second-order finite volume method". In *Proceedings of the 13th Spring Schoold on Transition and Turbulence*. ABCM.

de Azevedo, V.W., Denner, F., Evrard, F. and Paladino, E.E., 2021. "Performance evaluation of standard second-order finite volume method for dns solution of turbulent channel flow". *Journal of the Brazilian Society of Mechanical Sciences and Engineering*, Vol. 43, No. 11, pp. 1–15.

Denner, F. and van Wachem, B.G., 2014. "Fully-coupled balanced-force vof framework for arbitrary meshes with least-squares curvature evaluation from volume fractions". *Numerical Heat Transfer, Part B: Fundamentals*, Vol. 65, No. 3, pp. 218–255.

Frederix, E., Mathur, A., Dovizio, D., Geurts, B. and Komen, E., 2018. "Reynolds-averaged modeling of turbulence damping near a large-scale interface in two-phase flow". *Nuclear Engineering and Design*, Vol. 333, pp. 122–130.

Fulgosi, M., Lakehal, D., Banerjee, S. and De Angelis, V., 2003. "Direct numerical simulation of turbulence in a sheared air–water flow with a deformable interface". *Journal of fluid mechanics*, Vol. 482, pp. 319–345.

Hudaya, A.Z., Dinaryanto, O., Widyatama, A., Indarto and Deendarlianto, 2018. "Experimental study on interfacial friction factor of the air-water stratified two-phase flow in a horizontal pipe". In *AIP Conference Proceedings*. AIP Publishing LLC, Vol. 2001, p. 030007.

Lakehal, D., Reboux, S. and Liovic, P., 2005. "Sub-grid scale modelling for the les of interfacial gas-liquid flows". *Houille Blanche*, Vol. 6, No. 05, p. 1.

Le Clainche, S., Ferrer, E., Gibson, S., Cross, E., Parente, A. and Vinuesa, R., 2023. "Improving aircraft performance using machine learning: a review". *Aerospace Science and Technology*, p. 108354.

Liovic, P. and Lakehal, D., 2007. "Multi-physics treatment in the vicinity of arbitrarily deformable gas–liquid interfaces".

Journal of Computational Physics, Vol. 222, No. 2, pp. 504–535.

Lombardi, P., De Angelis, V. and Banerjee, S., 1996. "Direct numerical simulation of near-interface turbulence in coupled gas-liquid flow". *Physics of Fluids (1994-present)*, Vol. 8, No. 6, pp. 1643–1665.

López, J., Zanzi, C., Gómez, P., Zamora, R., Faura, F. and Hernández, J., 2009. "An improved height function technique for computing interface curvature from volume fractions". *Computer Methods in Applied Mechanics and Engineering*, Vol. 198, No. 33, pp. 2555–2564.

Moser, R.D., Kim, J. and Mansour, N.N., 1999. "Direct numerical simulation of turbulent channel flow up to re_τ= 590". *Physics of fluids*, Vol. 11, No. 4, pp. 943–945.

Petalas, N. and Aziz, K., 2000. "A mechanistic model for multiphase flow in pipes". *Journal of Canadian petroleum technology*, Vol. 39, No. 06.

Pope, S.B., 2001. "Turbulent flows".

Trofimova, A.V., Tejada-Martínez, A.E., Jansen, K.E. and Lahey Jr, R.T., 2009. "Direct numerical simulation of turbulent channel flows using a stabilized finite element method". *Computers & Fluids*, Vol. 38, No. 4, pp. 924–938.

Ubbink, O. and Issa, R., 1999. "A method for capturing sharp fluid interfaces on arbitrary meshes". *Journal of Computational Physics*, Vol. 153, No. 1, pp. 26–50.

Zonta, F., Onorato, M. and Soldati, A., 2016. "Decay of gravity-capillary waves in air/water sheared turbulence". *International Journal of Heat and Fluid Flow*, Vol. 61, pp. 137–144.

6. RESPONSIBILITY NOTICE

The authors are solely responsible for the printed material included in this paper.